Structural Characteristics of Dipalmitoylphosphatidylcholine and Hydrolysates from Sunflower Protein Isolate Mixed Monolayers Spread at the Air−Water Interface

José Miñones Conde,[†,‡] José Miñones Trillo,[‡] and Juan M. Rodríguez Patino*[,†]

Departamento de Ingeniería Química, Facultad de Química, Universidad de Sevilla, C/. Prof. García González, 1. 41012-Sevilla, Spain, and Departamento de Química Física, Facultad de Farmacia, Universidad de Santiago de Compostela, Campus Universitario Sur. 15706-Santiago de Compostela, Spain

Received: March 27, 2006; In Final Form: April 17, 2006

In this work, surface film balance and Brewster angle microscopy techniques have been used to analyze the structural characteristics (structure, topography, reflectivity, thickness, miscibility, and interactions) of hydrolysates from sunflower protein isolate (SPI) and dipalmitoylphosphatidylcholine (DPPC) mixed monolayers spread on the air−water interface. The degree of hydrolysis (DH) of SPI, low (5.62%), medium (23.5%), and high (46.3%), and the protein/DPPC mass fraction were analyzed as variables. The structural characteristics of the mixed monolayers deduced from the surface pressure (π)−area (A) isotherms depend on the interfacial composition and degree of hydrolysis. At surface pressures lower than the equilibrium surface pressure of SPI hydrolysate ($\pi_e^{\text{SPI hydrolysate}}$), both DPPC and protein are present in the mixed monolayer. At higher surface pressures (at $\pi > \pi_e^{\text{SPI hydrolysate}}$), collapsed protein residues may be displaced from the interface by DPPC molecules. The differences observed between pure SPI hydrolysates and DPPC in reflectivity (I) and monolayer thickness during monolayer compression have been used to analyze the topographical characteristics of SPI hydrolysates and DPPC mixed monolayers at the air−water interface. The topography, reflectivity, and thickness of mixed monolayers confirm at microscopic and nanoscopic levels the structural characteristics deduced from the $\pi-A$ isotherms.

Introduction

To stabilize food dispersions (emulsions and foams), emulsifiers (lipids, phospholipids, proteins, some polysaccharides, etc.) must be placed at the interface, so they can form a film around droplets or bubbles, respectively.[1,2] Proteins and low-molecular-weight emulsifiers (LMWEs, i.e., lipids and phospholipids) are often used simultaneously in food formulations, and knowledge of their interfacial physical−chemical characteristics, such as surface activity, structure, interactions, stability, dynamic phenomena, and interfacial rheological properties, and the kinetics of the film formation at fluid interfaces are important for the optimization of dispersion formation, stability, and texture.[1−8]

Mixtures of different emulsifiers (LMWEs and proteins) used in commercial food formulations often exhibit properties superior to those of the individual emulsifier alone due to synergistic interactions between emulsifier molecules.[3,6,7,9] Interactions between molecules of emulsifiers could affect not only the film structural characteristics[10−12] but also dynamic phenomena in mixed monolayers.[7,12−14] There are many experimental results available on the interfacial characteristics of milk protein and LMWE (lipids, phospholipids, or surfactants) mixed films at fluid interfaces.[3,4,6,7,9] However, as far as we know, there have been few studies of the interfacial characteristics of plant proteins and LMWE spread at the air−water interface,[15,16] although in practice mixtures of these emulsifiers are usually used in order to achieve an optimal effect in food formulations.[1,3,6,7,9]

The aim of this contribution was to analyze the structural characteristics (structure, topography, reflectivity, thickness, miscibility, and interactions) of mixed food emulsifiers (sunflower protein isolate (SPI) hydrolysates at different degrees of hydrolysis and dipalmitoylphosphatidylcholine (DPPC)) at the air−water interface. Monolayers at the air−water interface are interesting systems for studying two-dimensional nanostructures of amphiphilic substances. A recent important technological research area is the self-assembly of emulsifiers at an interface. Thus, the analysis in terms of molecular physical−chemical characteristics of food emulsifiers (mixtures) at fluid interfaces is of interest for a fundamental understanding of the engineering of food formulations (emulsions, foams, and gels).

The inclusion of phospholipids in addition to SPI can overcome the problems derived from an interfacial film with low protein−protein interactions (with low mechanical properties), as the small peptides produced during enzymatic hydrolysis dominate the interface at higher degrees of hydrolysis. On the other hand, the inclusion of a phospholipid in addition to SPI hydrolysates with high degrees of hydrolysis would be of interest for either enteral or parenteral formulations with biologically active hydrolysates or as a vehicle of choice for the delivery of specific hydrolysates. This application could significantly increase the value of the raw material (defatted sunflower meal) if it is utilized for the production of high-degree hydrolysates[17,18] for use in new processed food products (safe, high-quality health foods with good nutritional and therapeutic values). In fact, extensive hydrolysates are used in functional food formulations as nutritional supplements[17−21] and in special medical diets.[22−24] In addition, phospholipids have intrinsic properties (nutritional and therapeutic) and are a source of fatty acids, organic phosphate, and choline.[25,26] This attractive synergy between

* To whom all correspondence should be addressed. Phone: +34 95 4556446. Fax: +34 95 4556447. E-mail: jmrodri@us.es.
† Universidad de Sevilla.
‡ Universidad de Santiago de Compostela.

10.1021/jp061881k CCC: $33.50
Published on Web 05/24/2006

TABLE 1: Physicochemical Properties of Sunflower Protein Isolate

component	composition (%)
moisture	5.10 ± 0.83
ash	3.00 ± 0.08
protein content	82.81 ± 0.45
soluble sugars	0.22 ± 0.02
polyphenols	0.45 ± 0.08
others	8.60

TABLE 2: Solubility at pH 7 and Chemical Composition of Sunflower Protein Isolate and Protein Hydrolysates from Sunflower Protein Isolate at Different Degrees of Hydrolysis (DH)

	protein (%, w/w)	modified protein	solubility (%, w/w) at pH 7.0
isolate	82.8		27.9
SPI hydrolysate at DH = 5.62%	93.9	60.5	70.8
SPI hydrolysate at DH = 23.3%	80.8	83.9	86.2
SPI hydrolysate at DH = 46.3%	74.5	94.7	92.8

technology and physiology justifies the interest in phospholipids, hydrolysates, and bioactive peptides for the formulation of functional foods.

Materials and Methods

Materials. The isolation of sunflower proteins (SPI) from defatted sunflower meal, the preparation of sunflower protein hydrolysates with low (5.62%), medium (23.5%), and high (46.3%) degrees of hydrolysis (DH), the determination of solubility, and chemical characterization (including the determination of molecular masses by gel filtration chromatography, amino acid analysis by high-performance liquid chromatography, and chemical composition) have been described elsewhere.[27] The physical−chemical properties of sunflower protein isolate and the solubility and chemical composition of SPI and its hydrolysates are included in Tables 1 and 2, respectively.[27] Proteins represent the main component of SPI, but soluble sugars (0.22 wt %) and polyphenols (0.45 wt %) represent minor components. The protein concentration in the isolate and in protein hydrolysates is higher than that in the original sunflower meal (33.3 wt %) but decreases as the degree of hydrolysis increases. However, the modified protein increases with the degree of hydrolysis due to the action of the enzyme on native SPI. Solubility is lower for SPI than for its hydrolysates and increases with the degree of hydrolysis.

Dipalmitoylphosphatidylcholine (DPPC) was supplied by Sigma (>99%). This phospholipid was spread at the air−water interface in the form of a solution, using chloroform/ethanol (4:1, v/v) as a spreading solvent. Analytical grade chloroform (Sigma, 99%) and ethanol (Merck, >99.8%) were used without further purification. To form the monolayer, protein was spread in the form of a solution using water at pH 7 as a spreading solvent. The sample was stored at 4 °C, and all work was done without further purification. Samples for the interfacial characteristics of protein and DPPC mixed monolayers were prepared using Milli-Q ultrapure water and were buffered at pH 7, using Trizma [$(CH_2OH)_3CNH_2/(CH_2OH)_3CNH_3Cl$] as supplied by Sigma (>95%) without further purification. Sodium azide (Sigma) was added (0.05 wt %) as an antimicrobial agent. The ionic strength was 0.05 M in all of the experiments.

Surface Film Balance. Measurements of the surface pressure (π) versus mass area (A) were performed on a fully automated Langmuir-type film balance using a maximum through area of 562 cm^2, as described elsewhere.[10,11] Before each measurement, the film balance was calibrated at 20 °C. Mixtures of particular mass fractions—ranging between 0 and 1, expressed as the mass fraction of DPPC in the mixture (X_{DPPC})—were studied. Aliquots of aqueous solutions of SPI hydrolysates (0.96−1.24 mg/mL) at pH 7 were spread on the interface by means of a micrometric syringe. The same method as that discussed in a previous paper[28] was used for the spreading of SPI hydrolysates at the air−water interface. After the protein spreading, a time period of 30 min was allowed to elapse before DPPC spreading. Afterward, a DPPC solution in the chloroform/ethanol mixture (0.33 mg/mL) was spread at different points on the protein monolayer. A time period of 15 min was allowed for solvent evaporation. To ensure interactions and homogeneity, the mixed monolayer was compressed to near the collapse point of the mixture and then expanded immediately to avoid the collapse. After 30 min at the maximum area, measurements of compression−expansion cycles were performed with a 30 min waiting time between each compression−expansion cycle. The compression rate was 3.3 cm·min^{-1}, which is the highest value for which $\pi-A$ isotherms have been found to be reproducible in preliminary experiments with disordered[29] and globular[30] proteins. All $\pi-A$ isotherms were recorded continuously by a device connected to the film balance and then analyzed off-line. The mean deviation for three measurements was within ±0.5 mN/m for surface pressure and $\pm 0.250 \times 10^{-3}$ m^2/mg for area. The temperature was measured by a thermocouple located just below the air−water interface. The subphase temperature was controlled at 20 °C by water circulation from a thermostat, within an error range of ±0.5 °C.

Brewster Angle Microscope (BAM). A commercial Brewster angle microscope (BAM), BAM2, manufactured by NFT (Göttingen, Germany) was used to study the topography of the monolayer. The reflected beam passes through a focal lens, into an analyzer at a known angle of incident polarization, and finally to a CCD camera. Rotation of the analyzer allows the image contrast to be adjusted by varying the reflected polarization that is passing to the camera. If the emulsifier domain does not have a uniform reflectivity, this reflectivity changes with the analyzer angle. Thus, the optical anisotropy, which is typical for liquid-condensed (LC) structures due to crystalline-like domains being formed at the air−water interface,[31] can be visualized for different positions of the analyzer relative to the plane of incidence. Further characteristics of the device and operational conditions were described elsewhere.[29,31] The surface pressure measurements, area, and reflectivity or film thickness as a function of time were carried out simultaneously by means of a device connected between the film balance and BAM. These measurements were performed during continuous compression and expansion of the monolayer at a constant rate with different shutter speeds ranging from 1/50 s to 1/500 s. In previous works,[29,31] we have deduced that a shutter speed of 1/50 s is appropriate for the analysis of protein monolayers at the air−water interface at low surface pressures, but higher shutter speeds (1/250 or 1/500 s) are more appropriate for the analysis of protein monolayers at higher surface pressures. The reflectivity at each point in the BAM image depends on the local thickness and monolayer optical properties. These parameters can be measured by determining the light intensity at the camera and analyzing the polarization state of the reflected light.[29,31] At the Brewster angle, $I = C \cdot \delta^2$, where I is the reflectivity, C is a constant, and δ is the monolayer thickness.[32]

Equilibrium Surface Pressure. The equilibrium spreading pressure (π_e) is the maximum surface pressure to which a spread monolayer may be compressed before monolayer collapse.

TABLE 3: Equilibrium Surface Pressure (π_e) for DPPC[33] and SPI Hydrolysate[28] Spread Monolayers at the Air−Water Interface, at 20 °C and at pH 7

phospholipid	π_e (mN/m)
DPPC	47.0
SPI hydrolysate at DH = 5.62%	29
SPI hydrolysate at DH = 23.5%	22
SPI hydrolysate at DH = 46.3%	23

Knowledge of π_e is important because it represents the point at which spread monolayers become thermodynamically unstable with respect to the bulk liquid phase. Thus, at surface pressures higher than π_e, the monolayer is in a metastable state and subjected to relaxation phenomena because of the transformation of a homogeneous monolayer phase into a heterogeneous monolayer−collapse phase system. Equilibrium spreading pressures of DPPC and SPI hydrolysates at 20 °C were measured by the Wilhelmy plate method as described elsewhere.[28,33] These are included in Table 3.[28,33]

Results and Discussion

Structural Characteristics of SPI Hydrolysates and DPPC Monolayers at the Air−Water Interface. Monolayer structural characteristics can be obtained from $\pi-A$ isotherms. The $\pi-A$ isotherms for mixed monolayers of DPPC and SPI hydrolysates at DH = 5.62% (Figure 1), 23.5% (Figure 2), and 46.3% (Figure 3), at a mass fraction of DPPC in the mixture (X_{DPPC}) ranging between 0 and 1, and at 20 °C for monolayers spread on buffered water at pH 7, are shown in Figures 1−3.

Pure Component Monolayers. As expected,[34] DPPC monolayers present a structural polymorphism as a function of surface pressure (Figures 1A, 2A, and 3A). The compressional coefficient deduced from the slope of the $\pi-A$ isotherm, $\kappa = -(\delta\pi/\delta A)_T$ (data not shown), corroborates the existence of a structural polymorphism for DPPC monolayers. A liquid-expanded (LE) phase structure (at $\pi < 5$ mN/m), a first-order phase transition—the intermediate region of the lower slope—between the LE and liquid-condensed (LC) structures (at 5 mN/m $< \pi <$ 9 mN/m), a liquid-condensed structure (at $\pi > 9$ mN/m), and monolayer collapse at a surface pressure of about 59 mN/m were observed. This collapse pressure (of poor reproducibility) is higher than the equilibrium surface pressure ($\pi_e \approx 47$ mN/m). Thus, DPPC monolayers are in a metastable state at $\pi > \pi_e$.

The results of $\pi-A$ isotherms (Figures 1A, 2A, and 3A), together with the compressional coefficient (data not shown), confirm[28] that with SPI hydrolysate films two different states of condensation or structures (structures I and II) can be distinguished. At higher surface pressures, the monolayer collapses at a pressure higher than the equilibrium surface pressure,[28] which is indicated in Figures 1−3 by means of arrows. The values of π_e for SPI hydrolysates at DH = 5.62, 23.5, and 46.3% are 29, 22, and 23 mN/m, respectively. The surface pressure of the transition between structures I and II decreased when the degree of hydrolysis increased. This transition was observed at surface pressures of 14.7, 14.3, and 12.3 mN/m as the degree of hydrolysis increased from 5.62 to 23.5 to 46.3%, respectively. At low surface pressures ($\pi < \pi_t$), SPI may exist as trains or adopt an expanded loop conformation with all amino acid segments located at the interface (structure I). At higher surface pressures ($\pi > \pi_t$), and up to the equilibrium surface pressure, amino acid segments are extended into the underlying aqueous solution and adopt the form of more condensed loops and tails (structure II).[28,35−37]

Structure, Interactions, and Compatibility in Mixed Monolayers. Mixtures of particular mass fractions of DPPC and SPI hydrolysates—ranging between 0 and 1, expressed as the mass fraction of DPPC in the mixture (X_{DPPC})—were studied (Figures 1−3). From the $\pi-A$ isotherms for the mixed monolayers, it can be seen that the structural characteristics and

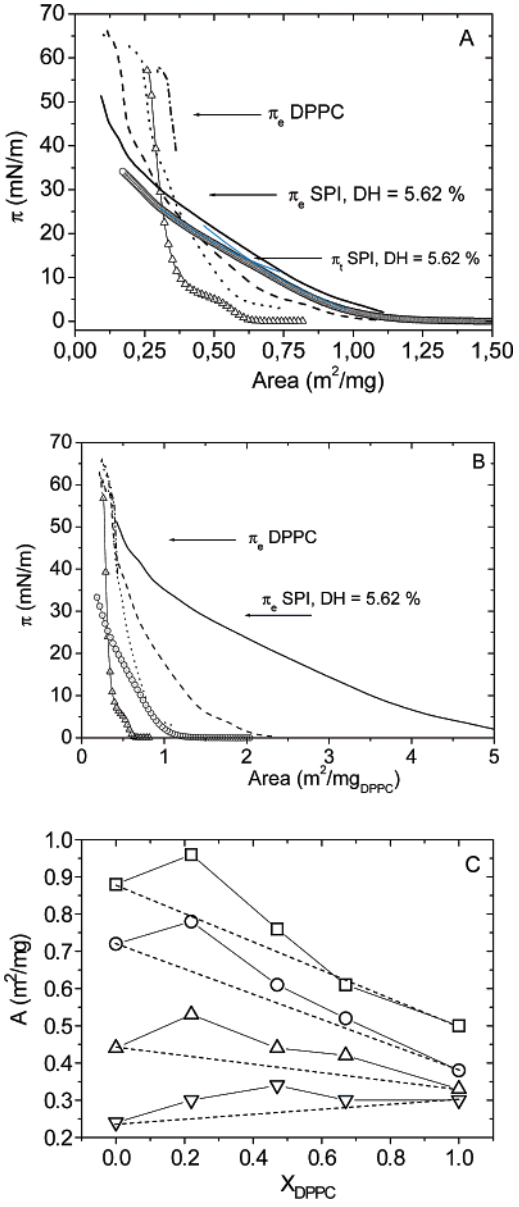

Figure 1. (A) Surface pressure−area isotherms (compression curves) for spread SPI hydrolysate at DH = 5.62% and DPPC mixed monolayers. The transition between structures I and II for SPI hydrolysate, deduced by the point of intersection of two lines drawn according to a virial equation,[41] is indicated by means of an arrow. (B) Surface pressure−area isotherms (compression curves) for spread SPI hydrolysate at DH = 5.62% and DPPC mixed monolayers. The molecular area for mixed monolayers was calculated on the basis that only DPPC was spread at the interface. The $\pi-A$ isotherm for pure SPI hydrolysate at DH = 5.62% was reproduced directly from part A. Symbols in parts A and B: mass fraction of DPPC in the mixture (X_{DPPC}), (○) 0, (—) 0.22, (- - -) 0.47, (••••) 0.67, (- • -) 0.83, and (△) 1.0. (C) Area as a function of mass fraction of DPPC in the mixture (X_{DPPC}) and surface pressure (mN/m): (□) 5, (○) 10, (△) 20, and (▽) 30. Temperature 20 °C, pH 7, and $I = 0.05$ M. The discontinuous line represents the mean area (A_i) calculated according to the additivity rule, $A_i = A_1 \cdot X_1 + A_2 \cdot X_2$, where A_1 and A_2 are the molecular areas of pure components and X_1 and X_2 are the mass fractions of pure components in the mixed monolayer. Thus, the excess area is $A_{exc} = A - A_i$. The π_e values of monolayer pure components are indicated by means of arrows.

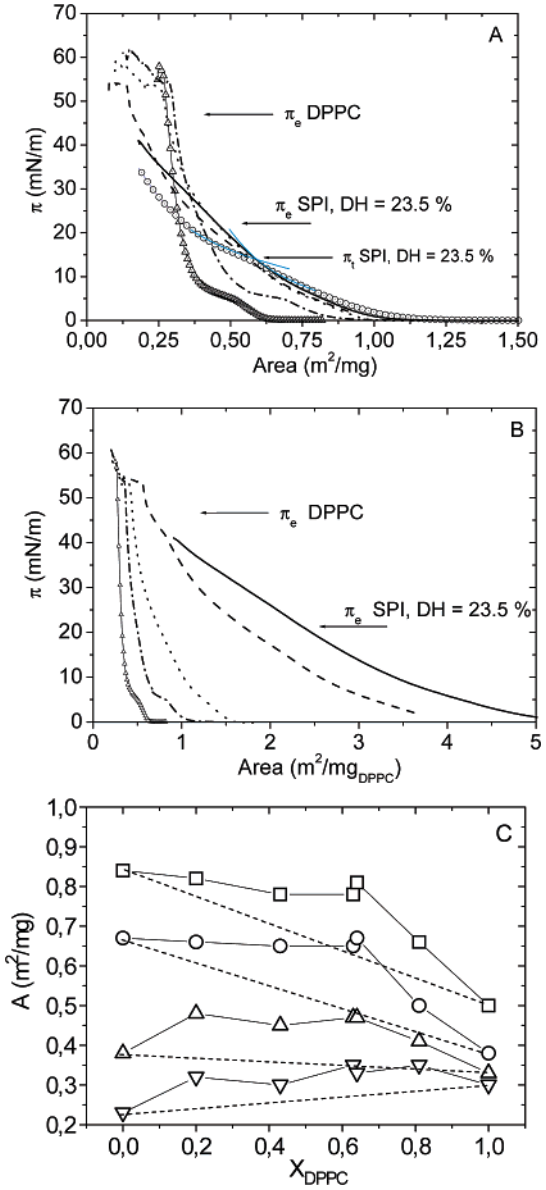

Figure 2. (A) Surface pressure−area isotherms (compression curves) for spread SPI hydrolysate at DH = 23.5% and DPPC mixed monolayers. The transition between structures I and II for SPI hydrolysate, deduced by the point of intersection of two lines drawn according to a virial equation,[41] is indicated by means of an arrow. (B) Surface pressure−area isotherms (compression curves) for spread SPI hydrolysate at DH = 23.5% and DPPC mixed monolayers. The molecular area for mixed monolayers was calculated on the basis that only DPPC was spread at the interface. The $\pi-A$ isotherm for pure SPI hydrolysate at DH = 23.5% was reproduced directly from part A. Symbols in parts A and B: mass fraction of DPPC in the mixture (X_{DPPC}), (○) 0, (—) 0.2, (- - -) 0.43, (••••) 0.64, (- • -) 0.81, and (△) 1.0. (C) Area as a function of mass fraction of DPPC in the mixture (X_{DPPC}) and surface pressure (mN/m): (□) 5, (○) 10, (△) 20, and (▽) 30. Temperature 20 °C, pH 7, and I = 0.05 M. The discontinuous line represents the mean area (A_i) calculated according to the additivity rule, $A_i = A_1 \cdot X_1 + A_2 \cdot X_2$, where A_1 and A_2 are the molecular areas of pure components and X_1 and X_2 are the mass fractions of pure components in the mixed monolayer. Thus, the excess area is $A_{exc} = A - A_i$. The π_e values of monolayer pure components are indicated by means of arrows.

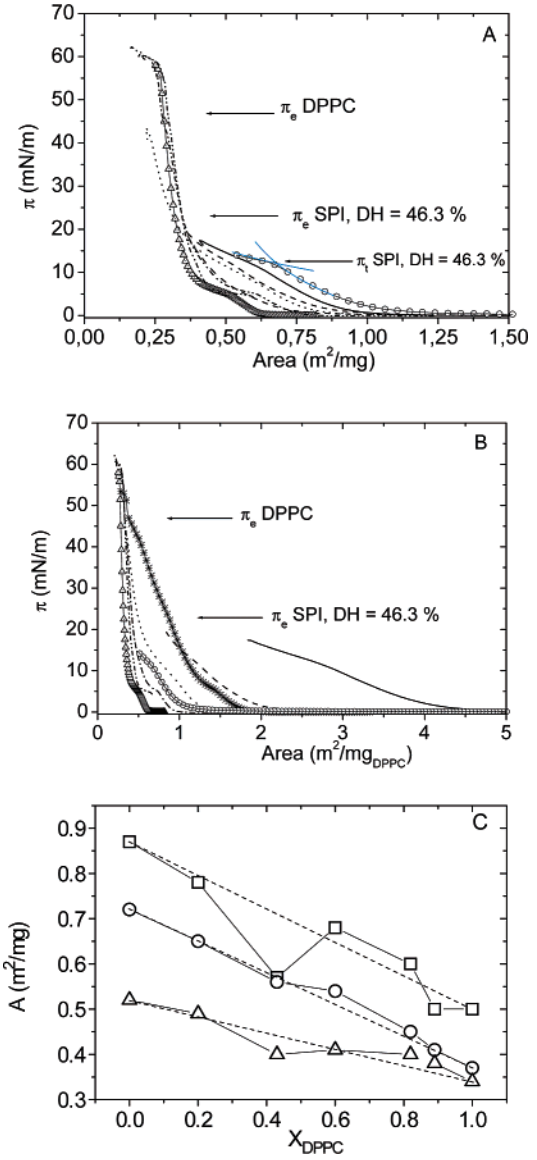

Figure 3. (A) Surface pressure−area isotherms (compression curves) for spread SPI hydrolysate at DH = 46.3% and DPPC mixed monolayers. The transition between structures I and II for SPI hydrolysate, deduced by the point of intersection of two lines drawn according to a virial equation,[41] is indicated by means of an arrow. (B) Surface pressure−area isotherms (compression curves) for spread SPI hydrolysate at DH = 46.3% and DPPC mixed monolayers. The molecular area for mixed monolayers was calculated on the basis that only DPPC was spread at the interface. The $\pi-A$ isotherm for pure SPI hydrolysate at DH = 46.3% was reproduced directly from part A. Symbols in (A) and (B): mass fraction of DPPC in the mixture (X_{DPPC}), (○) 0, (—) 0.2, (- - -) 0.43, (*) 0.5, (••••) 0.6, (- • -) 0.82, (- •• -) 0.89, and (△) 1.0. (C) Area as a function of mass fraction of DPPC in the mixture (X_{DPPC}) and surface pressure (mN/m): (□) 5, (○) 10, (△) 20, and (▽) 30. Temperature 20 °C, pH 7, and I = 0.05 M. The discontinuous line represents the mean area (A_i) calculated according to the additivity rule, $A_i = A_1 \cdot X_1 + A_2 \cdot X_2$, where A_1 and A_2 are the molecular areas of pure components and X_1 and X_2 are the mass fractions of pure components in the mixed monolayer. Thus, the excess area is $A_{exc} = A - A_i$. The π_e values of monolayer for pure components are indicated by means of arrows.

interactions between monolayer-forming components depend on the surface pressure and the degree of hydrolysis of SPI.

At surface pressures lower than the equilibrium surface pressures for SPI hydrolysates (at $\pi < \pi_e^{\text{SPI hydrolysate}}$) at DH = 5.62% (Figure 1A), 23.5% (Figure 2A), and 46.3% (Figure 3A), there was a monolayer expansion as the DPPC concentration in the mixture was decreased. That is, the $\pi-A$ isotherm was displaced toward higher areas as the concentration of DPPC in the mixture decreased. At these surface pressures (at $\pi < \pi_e^{\text{SPI hydrolysate}}$), both protein and DPPC coexist at the interface. In fact, from the $\pi-A$ isotherms and compressional coefficient,

one can see the same structural polymorphism as that for a pure DPPC monolayer at a high DPPC concentration in the mixture, but at low DPPC concentrations, the $\pi-A$ isotherms for mixed monolayers approach those for SPI hydrolysates and the transition between structures I and II can be distinguished. In summary, it can be concluded that the addition of DPPC to the SPI hydrolysate monolayer causes monolayer condensation and causes the disappearance of the transition between structures I and II, which is characteristic of pure proteins. However, it demonstrates the presence of the main transition between LE and LC phases, which is characteristic of DPPC monolayers.

At surface pressures higher than that for protein collapse (at $\pi > \pi_e^{\text{SPI hydrolysate}}$), the $\pi-A$ isotherms for mixed monolayers for SPI hydrolysates at DH = 5.62% (Figure 1A) and 23.5% (Figure 2A) were parallel to that of DPPC. However, the $\pi-A$ isotherm for mixed monolayers for SPI hydrolysates at DH = 46.3% (Figure 3A) practically matched that of pure DPPC. These data are in agreement with those deduced for spread milk protein and monoglyceride mixed monolayers.[7] These results suggest that at higher surface pressures (at $\pi > \pi_e^{\text{SPI hydrolysate}}$) the arrangement of the DPPC hydrocarbon chain in mixed monolayers is practically the same in the entire protein/DPPC ratio. This phenomenon may also be attributed to protein displacement by the DPPC from the interface.

In Figures 1B, 2B, and 3B, the hypothetical $\pi-A$ isotherms for mixed monolayers, calculated on the basis that only DPPC is present at the air−water interface, are shown. It must be emphasized that, due to this assumption, in these figures, the area on the *X*-axis is not the true area per unit mass of mixed monolayer but the apparent area. For this reason, the *X*-axes in Figures 1A, 2A, and 3A (for area per unit mass of mixed monolayer) are different from those in Figures 1B, 2B, and 3B (for apparent area per unit mass of DPPC in the mixture). It can be seen that, supposing that the mixed monolayers are dominated by DPPC, the $\pi-A$ isotherms for SPI hydrolysates at DH = 5.62% (Figure 1B) and 23.5% (Figure 2B) mixed monolayers, at $X_{\text{DPPC}} > 0.2$, and at $\pi > \pi_e^{\text{SPI hydrolysate}}$, are practically coincident and parallel to that of pure DPPC. For SPI hydrolysates at DH = 46.3% (Figure 3B), the coincidence between the $\pi-A$ isotherms for DPPC and mixed monolayers is practically total, even at surface pressures lower than $\pi_e^{\text{SPI hydrolysate}}$, at high concentrations of DPPC in the mixture. In contrast to the above data, the $\pi-A$ isotherms calculated on the basis that the mixed monolayers are dominated by the protein are totally different from those for pure components under all experimental conditions (data not shown). These data confirm the existence of protein displacement by the DPPC from the interface, which is facilitated as the degree of hydrolysis increases. That is, as the interactions between protein residues with lower molecular masses decreases at higher degrees of hydrolysis,[28] as a consequence of the enzymatic treatment,[27] protein displacement by DPPC from the air−water interface is facilitated.

Miscibility between Monolayer-Forming Components. The interactions between monolayer-forming components in mixed monolayers at $\pi < \pi_e^{\text{SPI hydrolysate}}$ can be studied from the point of view of miscibility by means of the excess area (A_{exc}). Figures 1C and 2C have shown positive values of excess area for DPPC and SPI hydrolysates at DH = 5.62% and at $X_{\text{DPPC}} \cong 0.2-0.6$ (especially at low surface pressures) and for DPPC and SPI hydrolysates at DH = 23.5% at every DPPC concentration of the mixed monolayers. These results and those deduced from $\pi-A$ isotherms prove that DPPC and SPI hydrolysates at DH = 5.62 and 23.5% form mixed monolayers at the air−water interface with few interactions between monolayer-forming components. It is conceivable to argue that these repulsive interactions may be of a steric character. The repulsive interactions in the mixed monolayer decrease as the surface pressure increases, as the monolayer-forming components adopt a similar liquidlike structure. Some electrostatic repulsion between DPPC and SPI hydrolysates is also possible at pH 7.[38] However, for DPPC and SPI hydrolysates at DH = 46.3% (Figure 3C), the excess area was practically zero, a phenomenon which proves that monolayer-forming components are immiscible at the air−water interface.

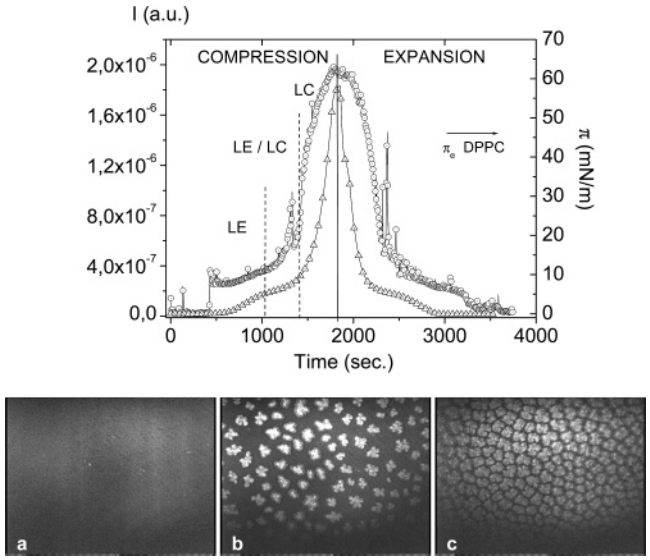

Figure 4. (top) Time evolution of reflectivity (○) and surface pressure (△) upon compression−expansion cycle for DPPC monolayer. The π_e value of DPPC (π_e DPPC) is indicated by an arrow. (bottom) Visualization by BAM of DPPC monolayers at (a) $\pi \approx 5$ mN/m, (b) $\pi = 6.4$ mN/m, and (c) $\pi > 30$ mN/m. The horizontal direction of the image corresponds to 630 μm and the vertical direction to 470 μm. Temperature 20 °C, pH 7.

At the highest surface pressures, at the collapse point of the mixed monolayer, immiscibility between monolayer-forming components is deduced[10,11] due to the fact that the collapse pressure of mixed monolayers is similar to that of a pure DPPC monolayer and does not depend on the monolayer composition (Figures 1A, 2A, and 3A).

The fact that, upon expansion and further compression, the $\pi-A$ isotherms were identical (data not shown) suggests that the protein reenters the mixed monolayer and supports the idea that the protein remains underneath the DPPC monolayer either through hydrophobic/electrostatic interactions between protein and DPPC or by local anchoring through the DPPC layer.[30,39]

Topographical Characteristics of DPPC and SPI Hydrolysate Monolayers at the Air−Water Interface. The results of the reflectivity and surface pressure as a function of time for pure DPPC monolayers (top of Figure 4) clearly show the same structural characteristics as those deduced from the $\pi-A$ isotherm. The reflectivity increases as the monolayer is compressed, passes through a maximum at the collapse point, and then decreases with monolayer expansion. The reflectivity curve for DPPC monolayer shows only a small increase of *I* at 5 mN/m, which is related to the LE−LC phase transition (Figure 4). In this case, the absence of reflectivity peaks, as well as the small values of reflectivity, indicates that the LE domains of DPPC are isotropic (Figure 4a). The value of *I* increases with monolayer compression and is a maximum at the collapse point. The reflectivity peaks observed during the monolayer compres-

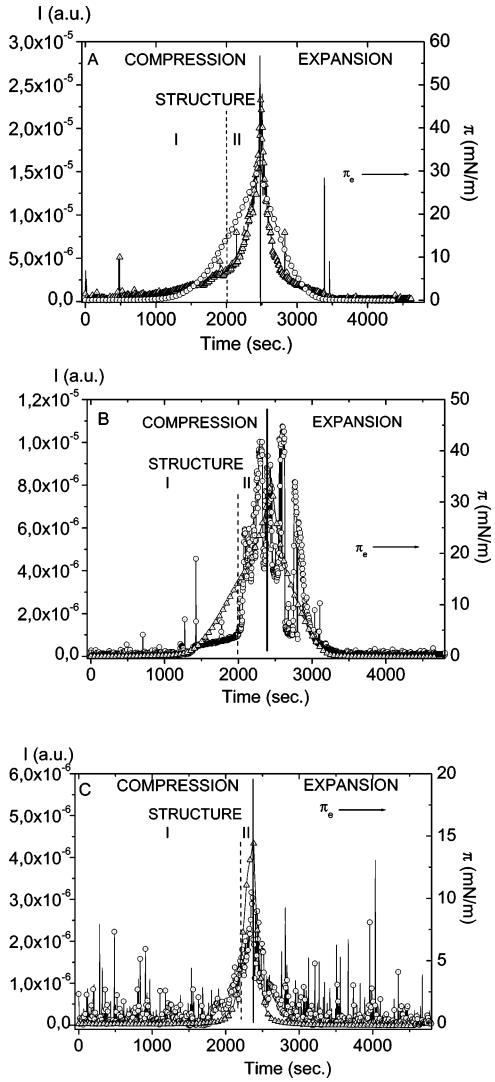

Figure 5. Time evolution of reflectivity (○) and surface pressure (△) upon compression−expansion cycle for SPI hydrolysates at DH: (A) 5.62%, (B) 23.5%, and (C) 46.3% monolayers spread at the air−water interface. Temperature 20 °C, pH 7, and $I = 0.05$ M. The π_e values are indicated by means of arrows.

sion with an LC structure were the consequence of the reflectivity when DPPC domains with LC structure (Figure 4b) pass through the spot where this measurement is performed.[40] These LC domains of DPPC grow in size and are more closely packed (Figure 4c) as the surface pressure increases.

For SPI hydrolysates, the reflectivity increases continuously during monolayer compression in the expanded regime (with structure I), in the condensed regime (with structure II), and becomes even higher at the collapse point (Figure 5). That is, an increase in monolayer reflectivity with surface pressure was produced, from the more expanded (structure I) to the more condensed (structure II) structure and a further increase at the monolayer collapse takes place. At the same surface pressure, the monolayer reflectivity was higher for SPI hydrolysates with lower degrees of hydrolysis (Figure 5). In fact, as the molecular masses of the protein fractions decrease at higher degrees of hydrolysis, as a consequence of the enzymatic treatment, the interactions between protein domains are lower and the monolayer reflectivity decreases.[27] In addition, the higher aggregation between protein microdomains in SPI hydrolysate at DH = 46.3%[28] produced reflectivity peaks in the monolayer topography (Figure 5C). That is, a more heterogeneous segregated monolayer was produced at the highest degree of hydrolysis.[28]

During monolayer expansion, similar phenomena as noticed upon compression are observed for either DPPC or SPI hydrolysate spread monolayers at the air−water interface (Figures 4 and 5). At a microscopic level, the compression−expansion cycle was practically reversible within the time of the experiment because the I−time curve during compression was practically the same as that during expansion.

The differences observed between pure SPI hydrolysates and DPPC in reflectivity during the compression−expansion cycle will be used in the next section to analyze the topographical characteristics of SPI hydrolysates and DPPC mixed monolayers at the air−water interface.

Effect of the Degree of Hydrolysis on the Topographical Characteristics of SPI Hydrolysates and DPPC Mixed Monolayers at the Air−Water Interface. Figures 6−8 show BAM images, at some representative mass fractions of DPPC in the mixture, and Figures 9−11 show the evolution of the reflectivity with surface pressure ($I-\pi$ plots) for compression of mixed monolayers of DPPC and SPI hydrolysates at DH = 5.62% (Figure 9), 23.5% (Figure 10), and 46.3% (Figure 11), as a function of the mass fraction of DPPC in the mixture (X_{DPPC}). For comparison purposes, continuous and discontinuous lines were deduced by fitting the $I-\pi$ data for single components, derived from different measurements. The reflectivity of SPI hydrolysate and DPPC mixed monolayers depends on the surface pressure and on the degree of hydrolysis.

Reflectivity of DPPC and SPI Hydrolysate Mixed Monolayers at Low Surface Pressures ($\pi < \pi_e^{\text{SPI hydrolysate}}$). For DPPC and SPI hydrolysate at DH = 5.62% and up to $\pi_e^{\text{SPI hydrolysate}}$, the reflectivity increases with surface pressure but does not depend on the monolayer composition, adopting values that are between those for pure components (Figure 9). These results confirm that under these experimental conditions DPPC and SPI hydrolysate at DH = 5.62% coexist at the interface with few interactions between them. In fact, BAM images (not shown) for mixed monolayers at $X_{DPPC} = 0.2$ and at low surface pressures (at $\pi < 10$ mN/m) demonstrate the presence of a homogeneous topography (as shown in Figure 4a), because both pure DPPC and SPI hydrolysate monolayers adopt an expanded structure (Figure 4). At higher surface pressures (between 10 and 30 mN/m), the presence of LC domains of DPPC can be observed in a homogeneous ambient of DPPC with LE structure and SPI hydrolysate (Figure 6a and b). The LC domains of DPPC (Figure 6b) and aggregation in SPI hydrolysate (Figure 6a) can also be well characterized by BAM images. In fact, it can be seen that for a position p of the analyzer relative to the plane of incidence of 60° the image in Figure 6c appears almost as an inverted image of that in Figure 6b in the absence of the analyzer. The optical anisotropy, as visualized by different positions of the analyzer, is typical for LC structures.[31] It should be noted that the morphology of the mixed monolayer in this region (Figure 6b and c) is significantly different from that for pure components. It can be seen that DPPC domain size (Figure 6b and c) is lower and domains do not appear with a characteristic shape, as for DPPC (Figure 4b), but as a network through the image, a phenomenon that can be associated with the presence of the hydrolysate in the mixed monolayers and probably with the existence of protein−lipid interactions. However, we do not reject the possibility that the presence of the viscoelastic SPI monolayer prevents nucleation and expansion of the SPPC liquid-condensed domains.

For DPPC and SPI hydrolysates at DH = 23.5% (Figure 10) and 46.3% (Figure 11) and up to $\pi_e^{\text{SPI hydrolysate}}$, the reflectivity increases with surface pressure but depends on the monolayer

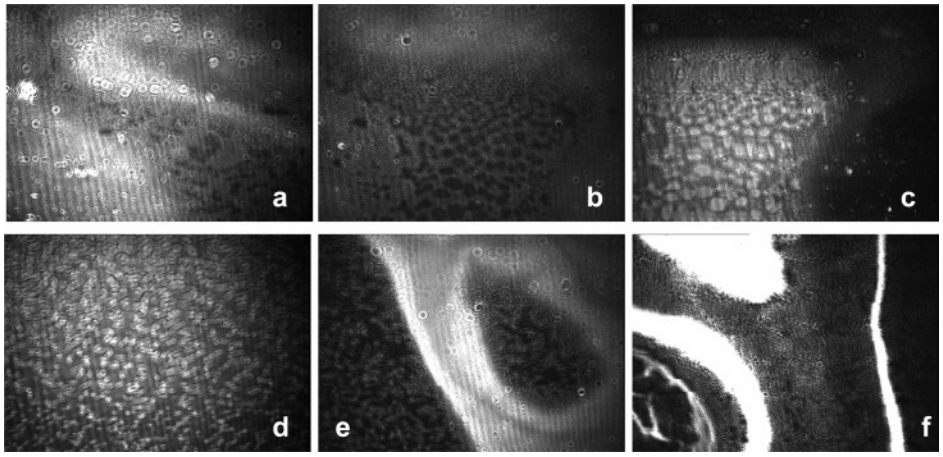

Figure 6. Visualization by BAM of (a) DPPC monolayers at $\pi \approx 5$ mN/m; the same image was observed for DPPC + SPI hydrolysate at DH = 5.62% mixed monolayers at $X_{DPPC} = 0.2$ and at 22.4 mN/m. (b) DPPC monolayers at $\pi = 6.4$ mN/m; the same image was observed for DPPC + SPI hydrolysate at DH = 5.62% mixed monolayers at $X_{DPPC} = 0.2$ and at 26.7 mN/m without analyzer. (c) DPPC monolayers at $\pi > 30$ mN/m; the same image was observed for DPPC + SPI hydrolysate at DH = 5.62% mixed monolayers at $X_{DPPC} = 0.2$ and at 22.4 mN/m for a position of the analyzer relative to the plane of incidence of 60°. DPPC + SPI hydrolysate at DH = 5.62% mixed monolayers at $X_{DPPC} = 0.2$ and at (d) 31 mN/m, (e) 34.8 mN/m, and (f) 41 mN/m. The horizontal direction of the image corresponds to 630 μm and the vertical direction to 470 μm. Temperature 20 °C, pH 7.

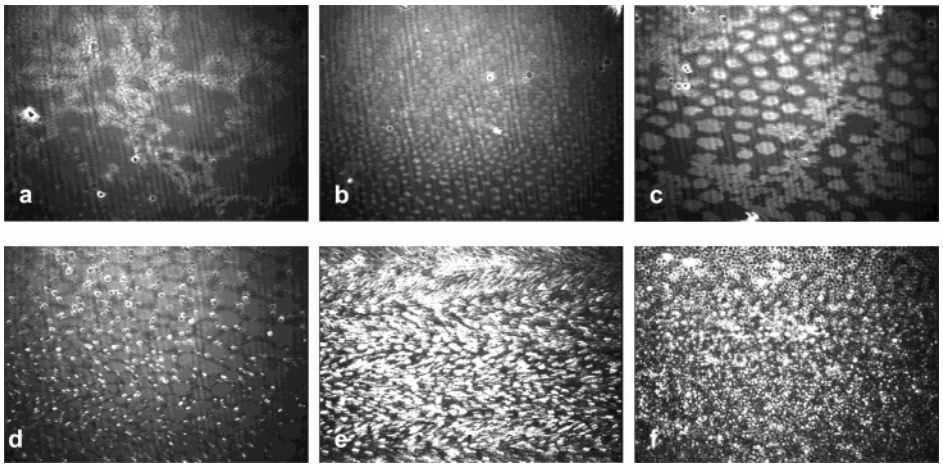

Figure 7. Visualization by BAM of DPPC + SPI hydrolysate at DH = 23.5% mixed monolayers at $X_{DPPC} = 0.5$ and at (a) $\pi = 4.9$ mN/m, (b) $\pi = 14.7$ mN/m, (c) $\pi = 17.5$ mN/m, (d) $\pi = 28$ mN/m, (e) $\pi = 37$ mN/m, and (f) $\pi = 41.4$ mN/m. Shutter speed 1/50 s. The horizontal direction of the image corresponds to 630 μm and the vertical direction to 470 μm. Temperature 20 °C, pH 7.

composition in a complicated manner. It can be seen that in general the reflectivity of the mixed monolayers is between that for pure components. However, for some mixtures, at specific surface pressures, the reflectivity of the mixed monolayer is higher than that for pure SPI hydrolysate monolayers. This is due to the fact that domains of collapsed SPI hydrolysates and DPPC which are formed during previous compressions of the mixed monolayer pass alternatively through the spot.

BAM images corroborate that for DPPC and SPI hydrolysates at DH = 23.5% (Figure 7) and 46.3% (Figure 8) at $\pi < \pi_e^{\text{SPI hydrolysate}}$ a mixed monolayer of DPPC and hydrolysate may exist with collapsed SPI hydrolysate and DPPC domains (Figures 7 and 8), which are formed during previous compressions of the mixed monolayer, in a homogeneous phase of pure components (Figure 8a and b) at the lowest π value. Small domains of DPPC (with a LC structure at $\pi > 5$ mN/m) uniformly distributed on the protein layer can also be distinguished in this region (Figure 7b). The LC domains of DPPC grow in size as the surface pressure increases (Figure 7c), as for pure DPPC monolayers. However, the topography of the mixed monolayer also proves the existence of some degree of interactions between monolayer-forming components because the regions of protein and LC domains of DPPC are not clearly separated (Figure 7c) due to the existence of some miscibility between them. The same phenomenon was observed for β-casein + phospholipids adsorbed films by atomic force microscopy, with a higher level of magnification.[38]

Reflectivity of DPPC and SPI Hydrolysate Mixed Monolayers at High Surface Pressures ($\pi > \pi_e^{\text{SPI hydrolysate}}$). At surface pressures higher than the π_e values of SPI hydrolysates (at $\pi > \pi_e^{\text{SPI hydrolysate}}$), the evolution of I with π follows a similar trend (with few exceptions) no matter what the degree of hydrolysis is (Figures 9−11). In this region, the reflectivity values of mixed monolayers are lower than those for SPI hydrolysates at $\pi_e^{\text{SPI hydrolysate}}$. A mixed monolayer of DPPC and SPI hydrolysate at DH = 46.3% and at $X_{DPPC} = 0.6$ is an exception (Figure 11). For this system, the reflectivity follows the same evolution with π as that for a pure SPI hydrolysate monolayer, adopting I values higher than those for DPPC, even at the collapse point of the mixed monolayer. Another exception was observed for the same system at $X_{DPPC} = 0.8$, because the reflectivity tends to that of a pure DPPC monolayer. The reflectivity peaks at some surface pressures (Figures 9−11) are due to the presence of aggregates of collapsed DPPC (with low

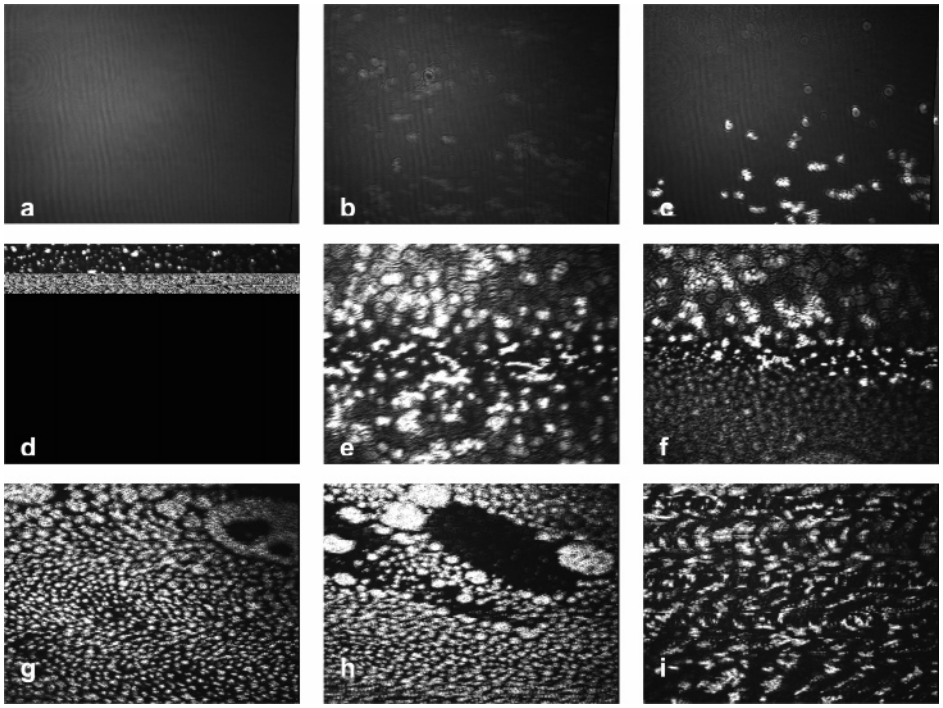

Figure 8. Visualization by BAM of DPPC + SPI hydrolysate at DH = 46.3% mixed monolayers at $X_{DPPC} = 0.5$ and at (a) $\pi \approx 0$ mN/m, (b) $\pi \approx 0.5$ mN/m, (c) $\pi \approx 1$ mN/m, (d) $\pi = 26.5$ mN/m, (e) $\pi = 33$ mN/m, (f) $\pi = 33$ mN/m, (g) $\pi = 35$ mN/m, (h) $\pi = 41.8$ mN/m, and (i) $\pi = 45$ mN/m. Shutter speed: (a−e) 1/50 s; (f−i) 1/120 s. The horizontal direction of the image corresponds to 630 μm and the vertical direction to 470 μm. Temperature 20 °C, pH 7.

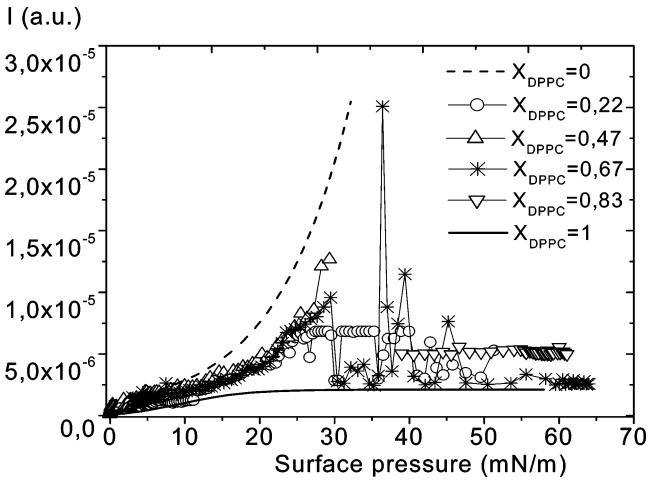

Figure 9. Effect of surface pressure on the reflectivity for SPI hydrolysate at DH = 5.62% and DPPC mixed monolayers during the compression (△). Mass fraction of DPPC in the mixture (X_{DPPC}): (- - -) 0, (○) 0.2, (△) 0.22, (*) 0.67, (▽) 0.83, and (—) 1. Shutter speed: 1/250 s. Temperature 20 °C, pH 7, and $I = 0.05$ M.

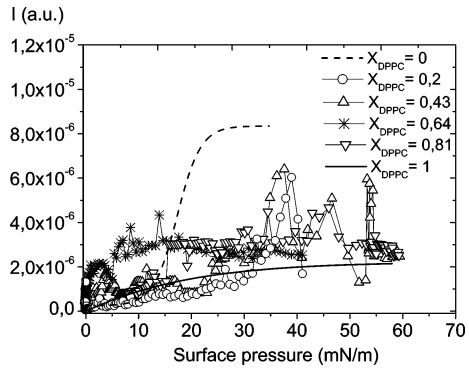

Figure 10. Effect of surface pressure on the reflectivity for SPI hydrolysate at DH = 23.5% and DPPC mixed monolayers during the compression (△). Mass fraction of DPPC in the mixture (X_{DPPC}): (- - -) 0, (○) 0.2, (△) 0.43, (*) 0.64, (▽) 0.81, and (—) 1. Shutter speed: 1/250 s. Temperature 20 °C, pH 7, and $I = 0.05$ M.

I) and collapsed hydrolysates (with high *I*) at the air−water interface. These results confirm that, at $\pi > \pi_e^{\text{SPI hydrolysate}}$, SPI hydrolysates are squeezed out by DPPC from the interface, but not totally. In fact, although in this region DPPC domains predominate at the interface, the existence of a sublayer of collapsed SPI hydrolysate causes a high reflectivity for mixed monolayers in comparison with that for a pure DPPC monolayer.

BAM images confirm the squeezing out of SPI hydrolysate by DPPC (Figures 6−8), as observed for other protein−monoglyceride mixed monolayers.[10,11,39] For SPI hydrolysate at DH = 5.62% and DPPC mixed monolayers, the squeezing out of the protein by DPPC can be clearly distinguished over a segregated region with dark LC domains of DPPC floating on bright collapsed protein (Figure 6d). At these surface pressures, there exist regions dominated by DPPC domains, which are so closely packed that the monolayer topography acquires a "high homogeneity" (Figure 6d). The squeezing out phenomenon of protein by DPPC was also observed in Figures 7e and f and 8d−i for mixed monolayers of DPPC and SPI hydrolysates at DH = 23.5 and 46.3%, respectively. However, the topography of mixed monolayers also proves the existence of some degree of interactions between monolayer-forming components and/or the prevention of nucleation and expansion of DPPC liquid-condensed domains by the presence of the viscoelastic SPI monolayer because the DPPC liquid-condensed domains in the mixed monolayer are of smaller size than those for a pure DPPC monolayer (see bottom of Figure 4). In addition, both regions are segregated and not clearly separated due to the existence of some miscibility between them. This monolayer segregation is characteristic of SPI hydrolysate at DH = 23.5 and 46.3%.

After a further compression, the presence of fractures in the monolayer with large domains of collapsed protein separating

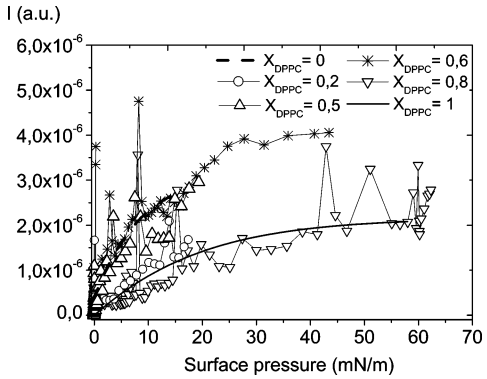

Figure 11. Effect of surface pressure on the reflectivity for SPI hydrolysate at DH = 46.3% and DPPC mixed monolayers during the compression (△). Mass fraction of DPPC in the mixture (X_{DPPC}): (- - -) 0, (○) 0.2, (△) 0.5, (*) 0.6, (▽) 0.8, and (—) 1. Shutter speed: 1/250 s. Temperature 20 °C, pH 7, and I = 0.05 M.

regions of DPPC with LC structure are typical features of SPI hydrolysate at DH = 5.62% (Figure 6e and f). Another topographical characteristic of the mixed monolayers—observed also in pure spread monolayers of SPI hydrolysate at DH = 23.5 and 46.3%[28]—was the presence of large fractures in the monolayer, from differences in illumination (Figure 8g and h), as the monolayer cracks cooperatively over large length scales, giving some regions of collapsed proteins separated by other regions with a lower condensation state.

Finally, at the collapse point of the mixed monolayers, the reflectivity is higher as compared with that for DPPC. These results demonstrated that in this region of highest surface pressures the DPPC is unable to displace all SPI hydrolysate molecules from the interface.

Thickness of DPPC and SPI Mixed Monolayers. From the $I-\pi$ curves, which reflect the nanoscopic surface equation of state of the spread material at the air−water interface (Figures 9−11), the evolution of the monolayer thickness with the surface pressure can be obtained. Figure 12 shows the evolution of the monolayer thickness during the compression of a pure DPPC monolayer and mixed monolayers of DPPC and SPI hydrolysates as a function of the degree of hydrolysis and at a representative DPPC concentration in the mixture (at X_{DPPC} = 0.5), as an example. The thicknesses of pure SPI hydrolysate monolayers[28] have been included as a reference.

The thickness of mixed monolayers of DPPC and SPI hydrolysates increased as the monolayer was compressed and was a maximum at the collapse point of mixed monolayers. That is, an increase in the thickness of the mixed monolayer with surface pressure was produced, from the more expanded to the more condensed structure, followed by a further increase at monolayer collapse, as for pure DPPC and SPI hydrolysate[28] monolayers. Although at surface pressures lower than $\pi_e^{\text{SPI hydrolysate}}$ the thickness of the mixed monolayer was practically the same as that of SPI hydrolysates, in the most condensed structure (especially at $\pi > \pi_e^{\text{SPI hydrolysate}}$), the thickness for mixed monolayers of DPPC and SPI hydrolysates tends to that of a pure DPPC monolayer, especially at the collapse point of the mixed monolayer (Figure 12).

These results confirm that at $\pi < \pi_e^{\text{SPI hydrolysate}}$ the presence of SPI hydrolysate dominates the thickness of the mixed monolayer but at $\pi > \pi_e^{\text{SPI hydrolysate}}$ the thickness of the mixed monolayer is dominated by the presence of DPPC. Interestingly, the presence of some fractures in mixed monolayers of SPI hydrolysate and DPPC at $\pi > \pi_e^{\text{SPI hydrolysate}}$, giving some regions of collapsed proteins separated by other regions with a lower condensation state (Figures 6−8), was reflected by drops in monolayer thickness at $\pi > \pi_e^{\text{SPI hydrolysate}}$ and, especially, near monolayer collapse (Figure 12).

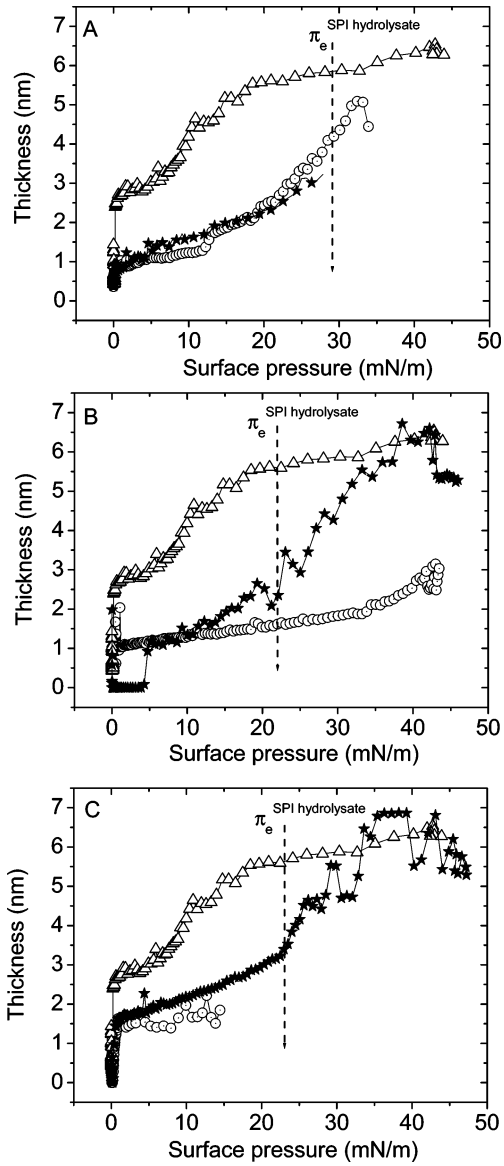

Figure 12. Effect of surface pressure on the monolayer thickness for (△) a pure DPPC monolayer and (*) mixed monolayers of DPPC and SPI hydrolysate at X_{DPPC} = 0.5 and at DH (A) 5.62%, (B) 23.5%, and (C) 46.3%, during the monolayer compression. The effects of surface pressure on the monolayer thickness for pure SPI hydrolysate monolayers (○) are included as a reference (Miñones et al. 2005b). The arrows indicate the values of the equilibrium surface pressures of spread monolayers of SPI hydrolysates ($\pi_e^{\text{SPI hydrolysate}}$). Temperature 20 °C, pH 7, and I = 0.05 M.

Conclusions

In this work, a surface film balance and Brewster angle microscopy have been used to analyze the structural characteristics (structure, topography, interfacial reflectivity, thickness, miscibility, and interactions) of mixed food emulsifiers (SPI hydrolysates at different degrees of hydrolysis and DPPC) at the air−water interface. DPPC monolayers present a structural polymorphism as a function of surface pressures. With SPI hydrolysate monolayers, two different structures (structures I and II) can be distinguished. The surface pressure of the transition between structures I and II decreased as the degree

of hydrolysis was increased. For DPPC and SPI hydrolysate mixed monolayers at $\pi < \pi_e^{\text{SPI hydrolysate}}$, the $\pi-A$ isotherm is displaced toward higher areas as the concentration of DPPC in the mixture decreases. At these surface pressures, both protein and DPPC coexist at the interface. At surface pressures higher than that for protein collapse (at $\pi > \pi_e^{\text{SPI hydrolysate}}$), there exists a displacement of protein by DPPC from the interface, which is facilitated as the degree of hydrolysis increases. The differences observed between pure SPI hydrolysates and DPPC in reflectivity (I) and in thickness during the monolayer compression can be used to analyze the topographical characteristics of SPI hydrolysates and DPPC mixed monolayers at the air−water interface. At low surface pressures (at $\pi < \pi_e^{\text{SPI hydrolysate}}$), the $I-\pi$ plot for the mixed monolayer was essentially the same, as for pure DPPC and SPI hydrolysate monolayers, due to the fact that both pure DPPC and SPI hydrolysate monolayers adopt an expanded structure. At higher surface pressures (at $\pi \approx \pi_e^{\text{SPI hydrolysate}}$), domains of pure SPI hydrolysate and DPPC were observed at the interface, with low interactions between them. After the SPI hydrolysate collapse, the reflectivity decreased to even lower values than those for DPPC. This suggests that in this region DPPC predominates at the interface, but DPPC is unable to displace all SPI hydrolysate molecules from the interface, even at the highest surface pressure (at the collapse point of the mixed monolayer). The evolution of thickness during the monolayer compression follows the same trend as the $I-\pi$ curves.

Many properties of food dispersions (stability, rheological and sensory characteristics, bioavailability of food constituents, etc.) depend on the dispersion microstructure, which is influenced by structural characteristics of adsorbed emulsifiers at fluid interfaces. In this work, we have observed at the microscopic and nanoscopic level that the structural characteristics of SPI hydrolysates and DPPC mixed films depend on the degree of hydrolysis and protein/DPPC ratio (property function). Moreover, the structural characteristics of the mixed films also depend on the surface pressure (process function). Thus, these results have implications for the formulation engineering (product engineering) of enteral or parenteral biologically active hydrolysates, for the design of a vehicle for delivery of specific hydrolysates with a high degree of hydrolysis, and in general for understanding interactions of phospholipids with proteins (polypeptides).

Acknowledgment. The authors acknowledge the support of CICYT through grants AGL2001-3843-C02-01 and AGL2004-01306/ALI. Drs. F. Millán and J. J. Pedroche (Instituto de la Grasa, C.S.I.C., Seville, Spain) are thanked for performing the preparation and characterization of sunflower protein isolate and its hydrolysates and for useful discussion concerning this project.

References and Notes

(1) Dickinson E. *An Introduction to Food Colloids*; Oxford University Press: Oxford, U.K., 1992.
(2) McClements, D. J. *Food emulsions: principles, practice and techniques*; CRC Press: Washington, DC, 1999.
(3) Dickinson, E. *Colloids Surf., B* **2001**, *20*, 197−210.
(4) Bos, M. A.; van Vliet, T. *Adv. Colloid Interface Sci.* **2001**, *91*, 437−471.
(5) Horne, D. S.; Rodríguez Patino, J. M. In *Biopolymers at interfaces*; Malmsten, M., Ed.; Marcel Dekker: New York, 2003; pp 857−900.
(6) Wilde, P. J. *Curr. Opin. Colloid Interface Sci.* **2000**, *5*, 176−181.
(7) Rodríguez Patino, J. M.; Rodríguez Niño, M. R.; Carrera, C. *Curr. Opin. Colloid Interface Sci.* **2003**, *8*, 387−395.
(8) Carrera, C.; Rodríguez Patino, J. M. *Food Hydrocolloids* **2005**, *19*, 407−416.
(9) Bos, M. T.; Nylander, T.; Arnebrandt, T.; Clark, D. I. In *Food emulsifiers and their applications*; Hasenhuette, G. L., Hartel, R. W., Eds.; Chapman & Hall: New York, 1997; pp 95−146.
(10) Rodríguez Patino, J. M.; Carrera, C.; Rodríguez Niño, M. R. *J. Agric. Food Chem.* **1999**, *47*, 4998−5008.
(11) Rodríguez Patino, J. M.; Carrera, C.; Rodríguez Niño, M. R. *Langmuir* **1999**, *15*, 4777−4788.
(12) Rodríguez Patino, J. M.; Rodríguez Niño, M. R.; Carrera, C.; Cejudo, M. *J. Colloid Interface Sci.* **2001**, *240*, 113−126.
(13) Rodríguez Patino, J. M.; Rodríguez Niño, M. R.; Carrera, C. *J. Agric. Food Chem.* **2003**, *51*, 112−119.
(14) Carrera, C.; Rodríguez Niño, M. R.; Rodríguez Patino, J. M. *Food Hydrocolloids* **2005**, *19*, 395−405.
(15) Damodaran, S.; Paraf, A. *Food Proteins and their Applications*; Marcel Dekker: New York, 1997.
(16) Örnebro, J.; Nylander, T.; Elisasson, A. C. *J. Cereal Sci.* **2000**, *31*, 195−221.
(17) Vioque, J.; Sánchez-Vioque, R.; Clemente, A.; Pedroche, J.; Millán, F. *J Am. Oil Chem. Soc.* **1999**, *76*, 819−823.
(18) Vioque, J.; Clemente, A.; Pedroche, J.; Yust, M. M.; Millán, F. *Grasas Aceites* **2001**, *52*, 132−136.
(19) Kilara, A.; Panyam, D. *Crit. Rev. Food Sci. Nutr.* **2003**, *43*, 607−633.
(20) Lahl, W. J.; Braun, S. D. *Food Technol.* **1994**, *48*, 68−71.
(21) Foegeding, E. A.; Davis, J. P.; Doucet, D.; McGuffey, M. K. *Trends Food Sci. Technol.* **2002**, *13*, 151−159.
(22) Cordle, C. T. *Food Technol.* **1994**, *48*, 72−76.
(23) Ziegler, F.; Ollivier, J. M.; Cynober, L.; Masinim, J. P.; Codray-Lucas, C.; Levis, E.; Giboudeau, J. *Gut* **1990**, *31*, 1277−1283.
(24) Clare, D. A.; Swaisgood, H. E. *J. Dairy Sci.* **2000**, *83*, 1187−1195.
(25) Cevec, G. *Phospholipids Handbook*; Marcel Dekker: New York, 1993.
(26) Golberg, I. *Functional Foods, Designer Foods, Pharmafoods, Nutraceuticals*; Chapman Hall: New York, 1994.
(27) Miñones, J., Jr.; Yust, M. M.; Pedroche, J. J.; Millán, F.; Rodríguez Patino, J. M. *J. Agric. Food Chem.* **2005**, *53*, 8038−8045.
(28) Miñones, J., Jr.; Miñones, J.; Rodríguez Patino, J. M. *Biomacromolecules* **2005**, *6*, 3137−3145.
(29) Rodríguez Patino, J. M.; Carrera, C.; Rodríguez Niño, M. R. *Food Hydrocolloids* **1999**, *13*, 401−408.
(30) Rodríguez Patino, J. M.; Carrera, C.; Rodríguez Niño, M. R.; Cejudo, M. *J. Colloid Interface Sci.* **2001**, *242*, 141−151.
(31) Rodríguez Patino, J. M.; Carrera, C. S.; Rodríguez Niño, M. R. *Langmuir* **1999**, *15*, 2484−2492.
(32) Azzam, R. M. A.; Bashara, N. M. *Ellipsometry and Polarized Light*; North-Holland: Amsterdam, The Netherlands, 1992.
(33) Miñones, J., Jr.; Rodríguez Patino, J. M. *Food Hydrocolloids*, in press.
(34) Miñones, J., Jr.; Miñones, J.; Conde, O.; Rodríguez Patino, J. M.; Dynarowicz-Latka, P. *Langmuir* **2002**, *18*, 2817−2827.
(35) Graham D. E.; Phillips, M. C. *J. Colloid Interface Sci.* **1979**, *70*, 427−439.
(36) Benjamins, J. Static and Dynamic Properties of Protein Adsorbed at Liquid Interfaces. Ph.D. Thesis, Wageningen University, Wageningen, 2000.
(37) Rodríguez Niño, M. R.; Carrera, C.; Pizones, V.; Rodríguez Patino, J. M. *Food Hydrocolloids* **2005**, *19*, 417−428.
(38) Lucero, A.; Rodríguez Niño, M. R.; Carrera, C.; Gunning, A. P.; Mackie, A. R.; Rodríguez Patino, J. M. In *Food Colloids: Interactions, Microstructure and Processing*; Dickinson, E., Ed.; Royal Society of Chemistry: Cambridge, U.K., 2005; pp 160−175.
(39) Rodríguez Patino, J. M.; Rodríguez Niño, M. R.; Carrera C.; Cejudo, M. *Langmuir* **2001**, *17*, 7545.
(40) Miñones, J., Jr.; Rodríguez Patino, J. M.; Conde, O.; Carrera, C.; Seoane, R. *Colloids Surf., A* **2002**, *203*, 273−286.
(41) Birdi, K. S. *Lipid and Biopolymers Monolayers at Liquid Interfaces*; Plenum Press: New York, 1989.